Xiao *et al. BMC Biotechnology* (2024) 24:60
https://doi.org/10.1186/s12896-024-00887-w

BMC Biotechnology

RESEARCH Open Access

A marker-free genetic manipulation method *for Glaesserella parasuis* strains developed by alternately culturing transformants at 37°C and 30°C

Jing Xiao[1,2], Yuxin Wang[1], Dongfang Wu[1,3], Yuping Song[1,2], Xuwang Cai[1,2], Huanchun Chen[1,2], Hongbo Zhou[1] and Xiaojuan Xu[1,2*]

Abstract

Background *Glaesserella parasuis* (*G. parasuis*) is the causative agent of Glässer's disease, which causes significant economic losses in the swine industry. However, research on the pathogenesis of *G. parasuis* has been hampered by the lack of a simple and efficient marker-free knockout system.

Results In this study, a marker-free knockout system was developed for *G. parasuis* using a temperature-sensitive vector. By alternating the incubation of transformants at 30°C and 37°C, we optimized the screening process for this system. The system was successfully applied to knockout the Kan^R cassette from JS0135Δ*nanH*::Kan^R, achieving a knockout efficiency of 90% in the final round of screening. To confirm that temperature variation was a key factor, we proceeded with knocking out the *nanH* and *apd* genes in the CF7066 strain. The knockout efficiency reached up to 100%, with the shortest screening time being only four days. The knockout of the *nanH* gene resulted in a significant reduction in the growth vitality of the strains, while the knockout of the *apd* gene led to an approximate 56% improvement in the adhesion rate. Additionally, we observed that the expression of recombinant genes in transformants was higher at 30℃ than at 37℃, with the *recC* gene being upregulated approximately 7-fold. In contrast, there was almost no difference in the expression of recombinant genes between 30℃ and 37℃ in the wild-type strains. This discrepancy was likely due to an elevated copy number of target plasmids at 30℃, which may have resulted in the enhanced expression of recombinant genes.

Conclusions In conclusion, this newly developed gene knockout system for *G. parasuis* presents a valuable tool for advancing research on this organism.

Keywords *G. Parasuis*, Homologous recombination, Temperature-sensitive plasmids, Marker-free knockout

*Correspondence:
Xiaojuan Xu
xuxiaojuan@mail.hzau.edu.cn
[1]State Key Laboratory of Agricultural Microbiology, College of Veterinary Medicine, Huazhong Agricultural University, Wuhan 430070, China
[2]Key Laboratory of Preventive Veterinary Medicine in Hubei Province, The Cooperative Innovation Center for Sustainable Pig Production, Wuhan 430070, China
[3]YuceBio Technology Co., Ltd, Shenzhen 518000, China

© The Author(s) 2024. **Open Access** This article is licensed under a Creative Commons Attribution-NonCommercial-NoDerivatives 4.0 International License, which permits any non-commercial use, sharing, distribution and reproduction in any medium or format, as long as you give appropriate credit to the original author(s) and the source, provide a link to the Creative Commons licence, and indicate if you modified the licensed material. You do not have permission under this licence to share adapted material derived from this article or parts of it. The images or other third party material in this article are included in the article's Creative Commons licence, unless indicated otherwise in a credit line to the material. If material is not included in the article's Creative Commons licence and your intended use is not permitted by statutory regulation or exceeds the permitted use, you will need to obtain permission directly from the copyright holder. To view a copy of this licence, visit http://creativecommons.org/licenses/by-nc-nd/4.0/.

Background

Glaesserella parasuis is a gram-negative bacterium belonging to the *Pasteurellaceae* family [1]. This organism is known to cause Glässer's disease, which is characterized by a constellation of symptoms, including fibrinous polyserositis, arthritis, meningitis, acute pneumonia, and septicemia [2–4]. Glässer's disease is a significant bacterial affliction of swine and has been reported on swine farms worldwide [5–7]. In China, the isolation ratio of *G. parasuis* was found to be as high as 22.6% in weaned swine and 9.7% in healthy swine herds [5, 8]. Therefore, gaining insight into the pathogenesis of Glässer's disease and understanding the interaction between *G. parasuis* and its host are crucial. To achieve this objective, it is essential to develop a marker-free gene knockout system.

Most strains of *G. parasuis* have been observed to possess highly stringent restriction-modification systems that impede the uptake of heterogeneous plasmids, particularly through electrotransformation [9, 10]. Consequently, allelic exchange knockout mutants of *G. parasuis* strains are frequently constructed using natural transformation with suicide plasmids. The plasmids contain antibiotic-resistance genes that are flanked by homologous regions upstream and downstream of the target gene that is to be deleted. Consequently, the resulting knockout mutants are marked with antibiotic-resistance [9, 11–13].

While marked mutants are valuable for investigating the molecular pathogenesis of *G. parasuis*, they may also exhibit antibiotic-resistance gene drift and other unpredictable polar effects. Moreover, these mutants are not suitable for use in commercial vaccines due to the presence of exogenous antibiotic-resistance genes. In our preliminary research, we established a markerless gene knockout system in *G. parasuis* based on the Flp-FRT system; however, it still leaves FRT sites on the genome [14]. Thus, a marker-free knockout approach is necessary for studying *G. parasuis* pathogenesis and developing genetically engineered vaccines. A *sacB*-based counter-selectable marker system has been applied to generate marker-free knockout mutants in *G. parasuis*; however, this method requires two natural transformations of two donor plasmids and is restricted to *G. parasuis* strains that lack spontaneous sucrose resistance [15].

In the present study, transformants carrying temperature-sensitive (TS) donor plasmids were cultured alternately at 37 °C and 30 °C to ensure genomic DNA replication and plasmid maintenance. Our results demonstrated successful knockout of target genes in different *G. parasuis* strains, leading to the establishment of a comprehensive marker-free gene knockout system for this organism.

Table 1 Strains and plasmids used in this study

Strains or plasmids	Genotype or characterization	Source or reference
Escherichia coli		
DH5α	F^-, φ 80d*lacZ*ΔM15, Δ(*lacZYA-argF*) U169, *deoR*, *recA1*, *endA1*, *hsdR17* (rK^-,mK^+), *phoA*, *supE44*, λ^-, *thi – 1*, *gyrA96*, *relA1*	TaKaRa Bio Inc., Dalian, China
Glaesserella parasuis		
SH0165	Wild-type, serotype 5	[22]
JS0135	Wild-type, serotype 4	This laboratory
JS0135Δ*nanH*::Kan^R	Δ*nanH*::Kan^R, generated via natural transformation of pK18-nHUD	This laboratory
CF7066Δ*nanH*-N	Δ*nanH*, constructed by *Ng*Ago deletion system	This study
JS0135Δ*nanH*	Δ*nanH*, constructed by temperature-sensitive system	This study
CF7066	Wild-type, serotype 5	This laboratory
CF7066Δ*nanH*	Δ*nanH*, generated via temperature-sensitive system	This study
CF7066Δ*apd*	Δ*apd*, generated via temperature-sensitive system	This study
Plasmids		
pK18 mobsacB	*pUC ori*, Kan^R, suicide vector of *G. parasuis*	[23]
pK18-nHUD	*pUC ori*, Kan^R, Δ*nanH*, from pK18 mobsacB, containing upstream and downstream regions of *nanH* to be deleted	This study
pSHK3-Gm	Gm^R, *pUC ori*, p*YC93 ori*, shuttle vector of *G. parasuis*	[18]
$pSHK3^{TS}$	Kan^R, *pUC ori*, *pA13* ori^{TS}, temperature-sensitive vector of *G. parasuis*	[17, 24]
pSHG5	Gm^R, *pUC ori*, *pA13* ori^{TS}	This study
pSHG5-Δ*nanH*	Gm^R, *pUC ori*, *pA13* ori^{TS}, Δ*nanH*	This study
pSHG5-Δ*apd*	Gm^R, *pUC ori*, *pA13* ori^{TS}, Δ*apd*	This study

Methods

Bacterial strains and growth conditions

The bacterial strains used in the study are listed in Table 1. *Escherichia coli* strain DH5α was grown in Luria–Bertani broth (LB; Difco, Detroit, MI, USA) or on LB agar. *G. parasuis* strains were grown in tryptic soy broth (TSB; Difco) or on tryptic soy agar (TSA; Difco) supplemented with 10 μg/mL NAD and 5% bovine serum. When needed, media were supplemented with kanamycin (50 μg/mL) or gentamicin (20 μg/mL). *G. parasuis* strains JS0135 (CCTCC AB 2021004) and CF7066 (CCTCC AB 2021003) were isolated in China and stored in our laboratory and at the China Center for Type Culture Collection. The original transformed recipient strain JS0135Δ*nanH*::Kan^R was generated through natural transformation with pK18-nHUD according to a previously published method [9]. The control mutant CF7066Δ*nanH*-N was constructed using a modified *Ng*Ago system [16] (Table 1).

Cell culture

Porcine kidney 15 (PK-15) cells were cultured in Dulbecco's modified Eagle's medium (DMEM, Gibco, USA) supplemented with 10% fetal bovine serum (FBS, Gibco, USA) at 37 °C with 5% CO_2.

Cloning and genetic manipulation

The plasmids used in this study are listed in Table 1. Primers for plasmid construction and mutant identification were designed based on the sequence of *G. parasuis* SH0165 (CP001321.1; Table S1). To construct the TS vector pSHG5, a fragment containing pUC ori and pA13 ori^{TS} was amplified from $pSHK3^{TS}$, and the gentamicin cassette was amplified from pSHK3-Gm [17, 18]. The resulting fragments were fused using a one-step cloning kit (Vazyme Biotech, Nanjing, China). For pSHG5-Δ*nanH*, the flanking homology arms of the deleted *nanH* allele of JS0135 (MT625975) were amplified using pK18-nHUD as a template and then ligated into pSHG5. For pSHG5-Δ*apd*, the flanking homology fragments of the deleted *apd* allele were obtained from *G. parasuis* CF7066 (MK617354) and fused to the pSHG5 vector using overlapping polymerase chain reaction (PCR) and a one-step cloning kit. Genetic constructs and PCR fragments were sequenced by Sanger sequencing (TsingKe Biotech, Beijing, China; Table 1, Table S1, and Fig. S1).

Electrotransformation of *G. Parasuis*

Electrotransformation of *G. parasuis* was performed according to a modified method of Lancashire et al. [19]. In brief, *G. parasuis* strains were grown on TSA plates at 37 °C for 12–14 h. Bacterial cells were then harvested in sucrose/glycerol (SG) buffer (15% [v/v] glycerol, 272 mM sucrose), washed three times, and resuspended in 0.12 mL SG buffer per sample. After electroporation (using a Bio-Rad MicroPulser Electroporator [Bio-Rad Laboratories, Hercules, CA, USA]; 2.5 kV, 0.2 cm cuvettes) with 5 μg plasmid DNA, cells were suspended in 1 mL TSB medium, grown at 37 °C for 2 h, and then spread on TSA plates supplemented with 20 μg/mL gentamicin.

Construction of marker-free knockout mutants in *G. Parasuis*

To generate crossover mutants, recipient strains were electroporated with donor plasmids and grown on gentamicin plates at alternating temperatures of 37 °C and 30 °C every 12 h. After several passages, single or double crossover colonies were screened by PCR using primers targeting the flanking regions of upstream and downstream homologous arms in the genome. Once a colony with a double crossover event was identified, it was cultured at 42 °C to cure the plasmid. To generate JS0135Δ*nanH* and CF7066Δ*nanH*, the double-crossover colony was further cultured at 42 °C until the optical density at 600 nm (OD_{600}) reached 0.5 and then spread on gentamicin-free TSA plates to isolate cells of different genotypes. For CF7066Δ*apd*, double-crossover colonies were directly streaked on TSA plates at 42 °C overnight and subsequently identified by PCR.

Detection of NanH and Apd using Western blotting

The expression of NanH and Apd in the wild-type and deletion strains was assessed by Western blotting using anti-NanH [20] and anti-Apd [21] mouse sera. Newly harvested bacterial cells were subjected to sodium dodecyl sulfate-polyacrylamide gel electrophoresis and then transferred to nitrocellulose membranes. After blocking and washing, the membranes were incubated with 1:5000 antisera specific for recombinant Apd and NanH in TBST buffer (20 mM Tris-HCl, 150 mM NaCl, 0.05% Tween 20, pH 7.4) containing 5% skim milk. The membranes were then exposed to horseradish peroxidase-labeled goat anti-mouse IgG (ABclonal, Inc., Wuhan, China) at a 1:5000 dilution in TBST buffer containing 5% skim milk, and the bound antibodies were visualized using Clarity Western ECL Substrate (Bio-Rad Laboratories).

Bacterial growth curve assays

The strains were activated on TSA plates for three generations, then single colonies were inoculated into 5 mL of TSB media, cultured with shaking at 37 °C/200 rpm for 12 h, and transferred to fresh TSB media at a 1:100 dilution. Next, 200 μL of bacterial solution was added to each well of the special detection plate suitable for the Bioscreen automatic growth curve analyzer. The OD_{600} of the bacterial solution was measured every 30 min, and the growth curve was recorded and plotted.

PK-15 cell adhesion and invasion assay

G. parasuis CF7066, JS0135 and the mutants were streaked on TSA plates and cultured at 37 °C for 16 h. The bacterial cells were then harvested on TSB media and the OD_{600} was adjusted to 1.0. PK-15 cells were grown to confluent monolayers in 24-well plates and infected with *G. parasuis* at a multiplicity of infection (MOI) of 0.02. The plates were centrifuged at 800 × g for 10 min to transport bacteria to the surface of the monolayer and incubated at 37 °C for 2 h. Thereafter, 100 μL medium and 900 μL ice water were added to each well and the plates were incubated at 4 °C for 15 min. The cells were then vigorously washed three times with PBS to eliminate nonspecific bacterial attachment and incubated for 15 min at 4 °C. The cells were then disrupted by repeated pipetting to liberate bacteria. Serial dilutions of the cell lysate were plated on TSA and incubated at 37 °C for 48 h. Adhesion rate = (Cell-associated CFU/Total

CFU) × 100. All assays were repeated at least three times in independent experiments.

Quantitative reverse-transcription PCR (qRT–PCR)

Total RNA was extracted from bacterial cells using a HiPure Bacterial RNA Kit (Magen, Guangzhou, China), and 1 μg of RNA was reverse transcribed into cDNA using a HiScript II Q RT SuperMix Kit (Vazyme Biotech, Nanjing, China) according to the manufacturer's protocol. qRT-PCR was performed using a ChamQ Universal SYBR qPCR Master Mix Kit (Vazyme Biotech, Nanjing, China) with the primers listed in Supplementary Table S1, and the results were normalized to those for GAPDH. The *G. parasuis* harboring plasmid pSHG5-Δ*apd* was streaked on TSA plates, divided into two groups and cultured at 37 °C or 30 °C. Bacterial cells were harvested and the OD_{600} was adjusted to 1.0. For each bacterial solution group, 1 μL of the sample was used for qRT-PCR. All assays were repeated at least three times in independent experiments.

Results

Knockout of the Kan^R cassette in JS0135ΔnanH::Kan^R

Given the potential resistance to endogenous gene knockout, we initially targeted the exogenous Kan^R gene in JS0135Δ*nanH*::Kan^R for knockout. The resulting Kan^R knockout strain did not exhibit growth defects compared to the parental strain JS0135Δ*nanH*::Kan^R, facilitating subsequent mutant screening. Therefore, we used the natural transformation method as previously described to replace the *nanH* gene with Kan^R in the *G. parasuis* strain JS0135, generating the marked mutant JS0135Δ*nanH*::Kan^R.

To knock out the Kan^R gene, the donor plasmid pSHG5-Δ*nanH* carrying the homologous arms of *nanH* was electroporated into JS0135Δ*nanH*::Kan^R. However, due to the abundant restriction-modification systems in JS0135, the strain exhibited strong resistance to electroporation, resulting in the generation of only one transformant without recombination after multiple attempts (Fig. 1a and b). Notably, the colonies grew better at 37 °C, but the temperature-sensitive plasmid pSHG5-Δ*nanH* could only replicate properly at or below 30 °C. To accommodate different temperatures requirements, the transformants were incubated for 2 days on gentamicin TSA plates at 37 °C, then streaked on fresh gentamicin TSA plates and cultured alternately at 37 °C and 30 °C for one passage (24–48 h). Newly grown single colonies were picked and cultured in the same manner for another generation. After five generations, we found that most colonies exhibited multiple genotypes (Fig. 1c). The bands observed in the gel correspond to four genotypes of JS0135 mutants: the 3239 bp band represents the parent strain genotype (Δ*nanH*::Kan^R) without recombination; the 2330 bp band represents the knockout mutant genotype (Δ*nanH*) resulting from double crossover with the parent strain; and the 6650/10,061 bp bands represent the single/twice crossover genotypes where the plasmid integrated into the parent strain genome via the upstream or downstream homologous arms (Fig. 1a and c). Interestingly, a faint band near the single crossover band (6650 bp) was observed after inverting the image colors, speculated to correspond to plasmid integration into the knockout mutant genome (Fig. S2).

To further screen for the knockout mutant, we selected colony No. 4 (Fig. 1c), which exhibited a relatively bright band for the double-crossover genotype. After inoculating this colony into gentamicin-free TSB and culturing it to the logarithmic growth phase, the cells were spread on gentamicin-free TSA plates at 42 °C. This approach successfully isolated Kan^R knockout colonies, with 90% of the colonies displaying the Kan^R cassette knockout genotype as the only genotype (Fig. 1d). The double and single crossover PCR fragments were then purified and confirmed through Sanger sequencing (Fig. 1e and Fig. S3).

Knockout of the *nanH* gene in wild-type CF7066

A previous study by our laboratory failed to screen mutants at 30 °C using a traditional temperature-sensitive plasmid method (unpublished). However, in this study, we successfully screened mutants and observed numerous recombinant genotypes. We speculated that the success of this method was due to the alternating culture temperatures of the transformants. To further confirm that alternating culture temperatures at 37 °C and 30 °C contributed to the accumulation of recombinants, we electroporated CF7066 with the pSHG5-Δ*nanH* plasmid and cultured it on gentamicin plates with alternating temperatures every 12 h. Among 21 randomly picked transformants, colonies No. 1 and 14 exhibited a single crossover genotype (5929 bp), and the other transformants were wild-type (2518 bp) (Fig. 2a and b).

As anticipated, colony No. 1 (Fig. 2b), which underwent alternating streaking at 37 °C and 30 °C, yielded the *nanH* knockout genotype (1610 bp) after eight passages (Fig. 2c). Colony No. 21 (Fig. 2c) showed the brightest band corresponding to the Δ*nanH* genotype. Further culturing of this colony allowed successful isolation of *nanH* knockout colonies using the described method (Fig. 2d). Consequently, the *nanH* knockout genotype was present in 7.6% (8/105) of the colonies (Fig. 2d and Fig. S4). Sanger sequencing confirmed the successful knockout of *nanH* (Fig. 2e).

In contrast to the JS0135Δ*nanH* generation, where most colonies exhibited the knockout genotype (Fig. 1d), most colonies in the CF7066Δ*nanH* screen restored the wild-type genotype (Fig. 2d and Fig. S4). This difference may be attributed to the growth advantage of the

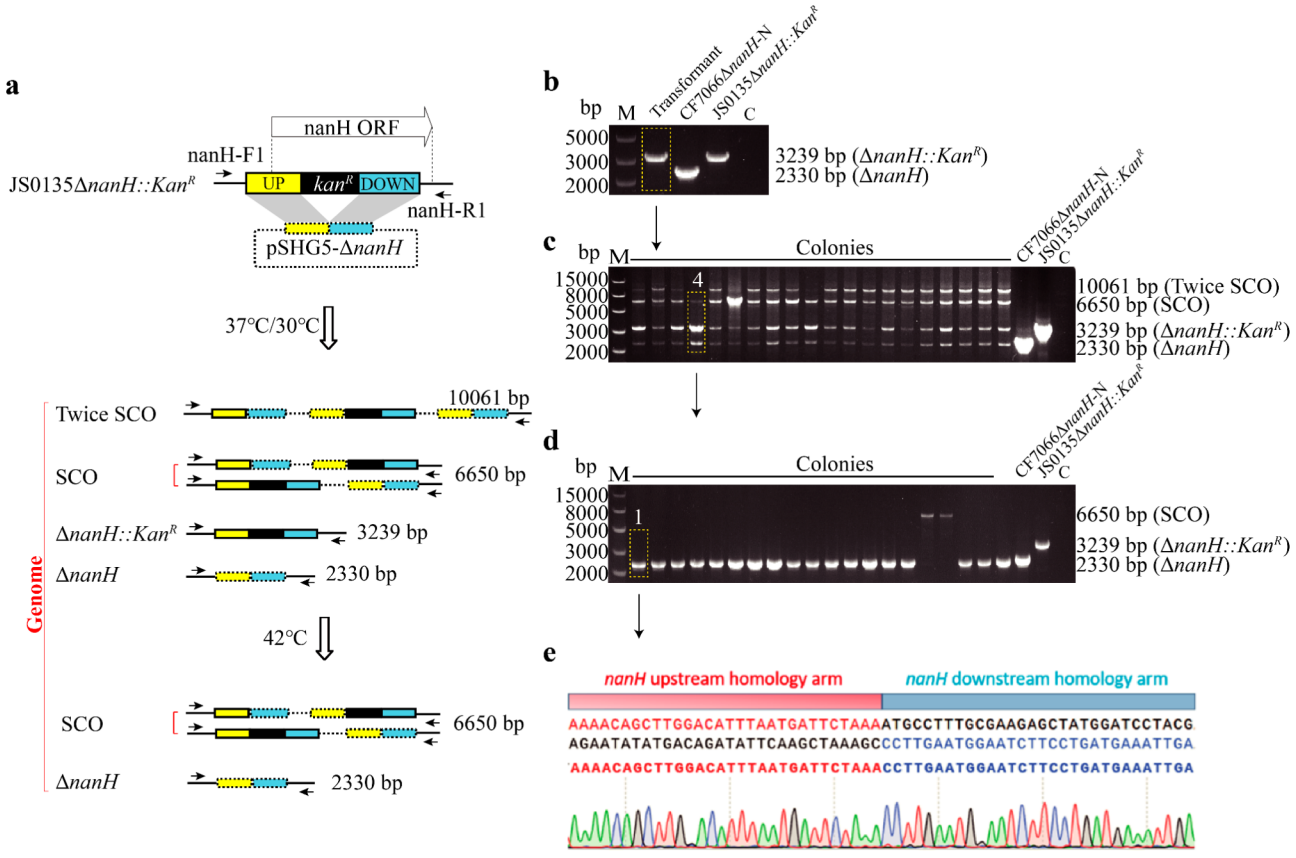

Fig. 1 Knockout of the *Kan*^{R} cassette from the marked mutant JS0135Δ*nanH::Kan*^{R}. (**a**) Schematic diagram illustrating the process for generating the marker-free mutant JS0135Δ*nanH* from the marked mutant JS0135Δ*nanH::Kan*^{R}. SCO, the single crossover genotype with one entire plasmid integrated into the genome. (**b**) Only one transformant grew, and PCR analysis using primers nanH-F1/R1 flanking the upstream and downstream homologous arms of *nanH* (3239 bp) showed that this transformant had no genotype change compared to JS0135Δ*nanH::Kan*^{R}. The *nanH* knockout mutant, CF7066Δ*nanH*-N, generated by the *Ng*Ago gene deletion system, served as the positive control. C, negative control. (**c**) Multiple genotypes (2330, 3239, 6650, and 10061 bp) were observed in progeny colonies after culturing alternately at 30 °C and 37 °C for five generations and were then screened by colony PCR analysis. Colony No. 4 was selected for culture at 42 °C for two passages using the process described above. (**d**) The marker-free *nanH* knockout mutants (2330 bp) were detected in 90.0% (18/20) of colonies. (**e**) Sanger sequencing was conducted to confirm the elimination of the antibiotic-resistance marker

dominant genotype. Specifically, JS0135Δ*nanH* outperformed JS0135Δ*nanH::Kan*^{R} because the expression of *Kan*^{R} did not affect growth on non-selective plates but imposed an additional growth burden. Similarly, the absence of *nanH* in CF7066Δ*nanH* might have impaired strain metabolism, giving CF7066 a growth advantage over CF7066Δ*nanH*. This growth advantage likely intensified during the subculture process.

Open reading frame (ORF) knockout contributes to the screening of mutants

To further confirm our hypothesis, we attempted to knock out the *apd* gene of CF7066 using the same method. To address potential difficulties in screening knockout colonies due to growth disadvantages, we improved the design of the donor plasmid pSHG5-Δ*apd* by placing the upstream and downstream homologous arms outside the ORF of *apd*. This design ensures that even if the transformant undergoes gene recombination resulting in the knockout of *apd* in the genome, the Apd protein can still be expressed from the plasmid.

The plasmid pSHG5-Δ*apd* was electroporated into CF7066 and cultured on gentamicin plates at 37 °C. Among the 22 transformants tested by colony PCR analysis, 21 produced a band corresponding to the wild-type genome (3958 bp). However, colony No. 17 produced a band indicative of the knockout genotype (1448 bp; Fig. 3a and b). After streaking this transformant on gentamicin-free plates at 42 °C for one passage, 7 progeny colonies were identified as the *apd* knockout genotype (Fig. 3c). Subsequently, colony No. 8 was streaked on gentamicin-free plates at 42 °C for a second passage, and the *apd* knockout genotype appeared in 100% of the progeny colonies tested (Fig. 3d and Fig. S5). Sanger sequencing was performed to further confirm the deletion of *apd* (Fig. 3e).

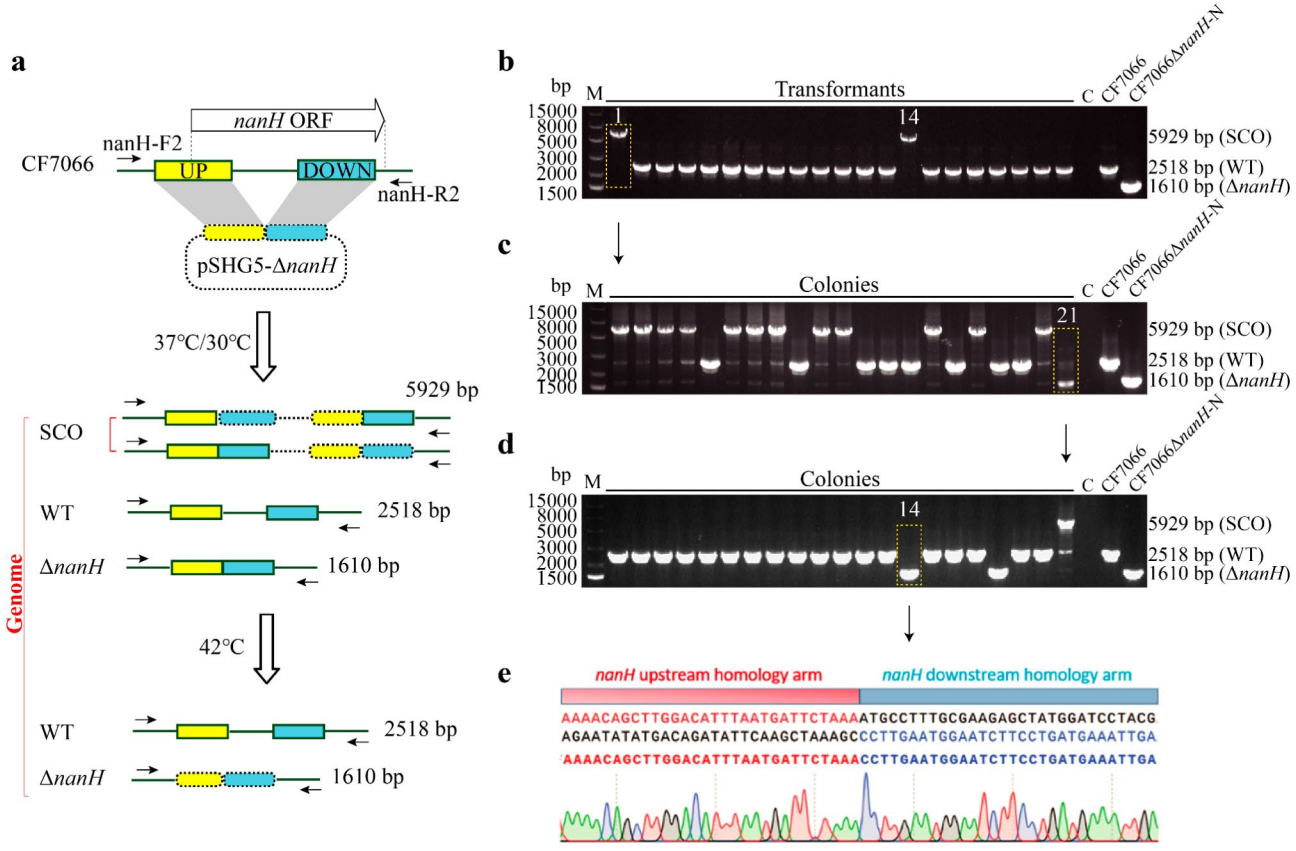

Fig. 2 Generation of marker-free in-frame knockout in *G. parasuis* CF7066. (**a**) Schematic diagram illustrating the process for generating an in-frame *nanH* knockout mutant. WT, wild-type *G. parasuis* CF7066. (**b**) The genotypes of transformants were amplified using primers nanH-F2/R2, which flank the upstream and downstream homologous arms of *nanH*. Two transformants contained a single crossover genotype (5929 bp), while the others retained the wild-type genotype (2518 bp). CF7066Δ*nanH*-N, the *nanH* knockout mutant generated by the *Ng*Ago deletion system. (**c**) Three genotypes were observed in progeny colonies after culturing colony No. 1 alternately at 37 °C and 30 °C for eight passages. Subsequently, colony No. 21, which exhibited the brightest knockout band (1620 bp), was selected and cultured at 42 °C for two passages. (**d**) Two colonies exhibited the *nanH* knockout genotype (1620 bp). (**e**) Sanger sequencing was conducted to confirm the marker-free in-frame *nanH* knockout in CF7066

During the process, the plasmid genotypes of the transformants were also detected by PCR using primers targeting the plasmid backbone that flanked the upstream and downstream homologous arms of *apd* (Fig. 3a). Of the 22 transformants tested, 14 contained pSHG5-Δ*apd* carrying the deleted *apd* allele (1130 bp), while 6 possessed the plasmid carrying the wild-type *apd* allele (3660 bp) (Fig. 3b). This result suggested that it might be necessary to examine the homology arms on the plasmid in the primary transformants to ensure that they had not been swapped with the genome. After colony No. 8 was cultured on gentamicin-free plates for one passage, 72.7% of the progeny colonies were cured (Fig. 3c and d). Compared to the previous two mutants JS0135Δ*nanH* and CF7066Δ*nanH*, the screening of CF7066Δ*apd* required only two passages, which considerably reduced the time required for mutant construction.

Biological characteristics of the three mutants

Target gene knockout was confirmed through Western blotting. In the wild-type strains JS0135 and CF7066, NanH expression was detectable, but absent in the JS0135Δ*nanH* and CF7066Δ*nanH* knockout mutants (Fig. 4a and b). Similarly, Apd was expressed in the wild-type CF7066 strain but not in the mutant CF7066Δ*apd* strain (Fig. 4c). These results provide further evidence that the TS plasmid-based procedure successfully generated marker-free deletion mutants of *G. parasuis*.

The phenotype, growth and adhesion of the strains were also detected. The growth curve presented in Fig. 4d showed that the deletion of *apd* had no significant effect on the growth of CF7066, while the deletion of *nanH* significantly inhibited the growth of CF7066 and JS0135. Additionally, the deletion of *apd* led to a significant increase in the bacterial adhesion rate of CF7066 compared to the wild-type strain, whereas the absence of *nanH* in CF7066 and JS0135 did not result in any noticeable differences compared to their respective wild-type

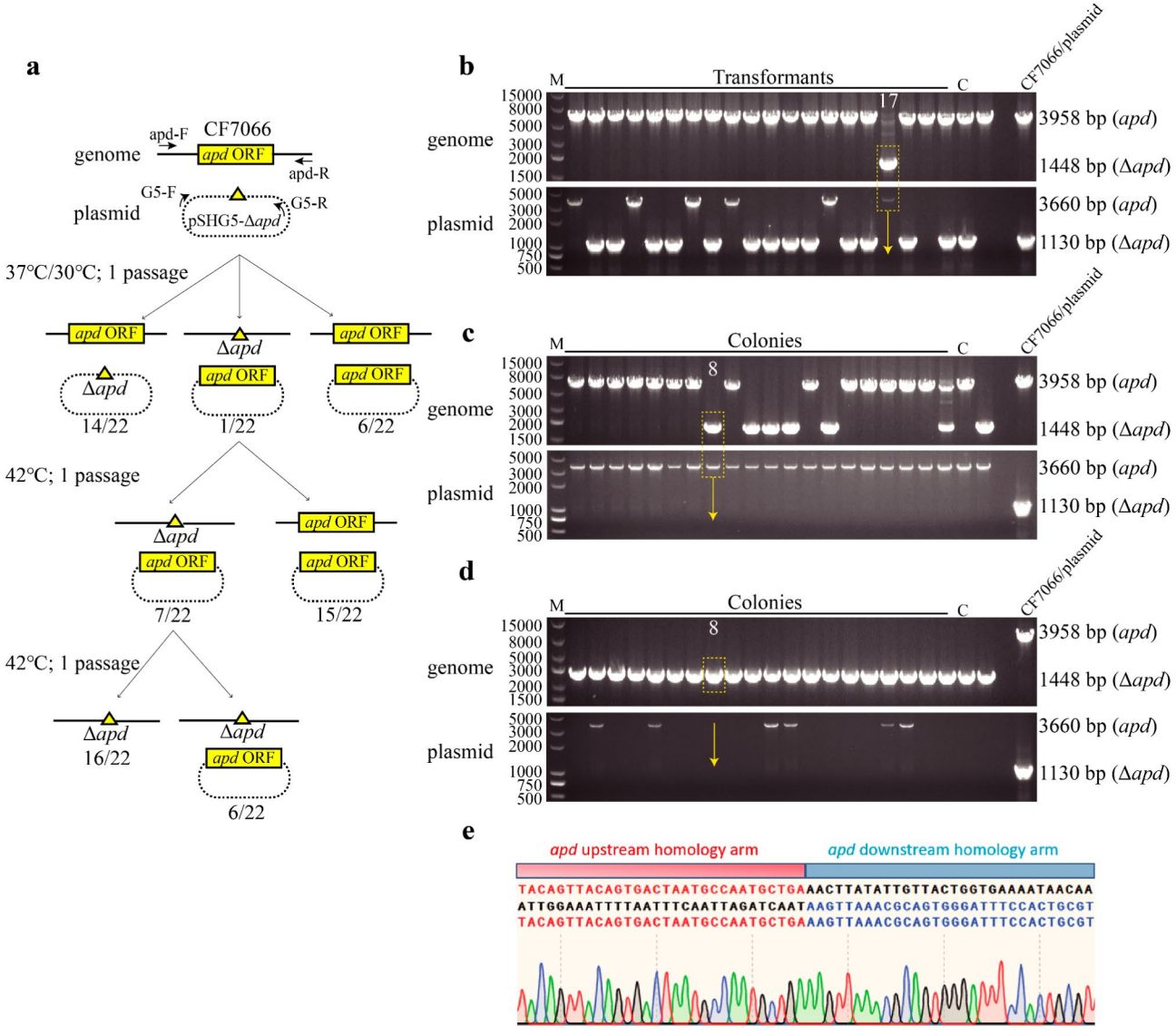

Fig. 3 Generation of an ORF knockout in *G. parasuis* CF7066. (**a**) Schematic diagram illustrating the process for generating the *apd* ORF knockout mutant. The plasmid pSHG5-Δ*apd* harbored the upstream and downstream homologous arms of *apd*, with the promoter and stop codon respectively. Three patterns of plasmid and genome genotype combinations in one colony are shown, with the proportion of each pattern among the 22 colonies indicated below the patterns. (**b**) After culturing the transformed bacteria alternately at 37 °C and 30 °C for one passage, the knockout genotype (1448 bp) appeared in the bacterial genome of colony No. 17, and the wild-type *apd* gene (3660 bp) was replaced by the Δ*apd* gene in the plasmids. (**c**) Colony No. 17 was streaked on gentamicin-free plates for one passage, and 7 out of 22 progeny colonies possessed the *apd* knockout genotype, while plasmids with the wild-type *apd* allele appeared in all colonies. (**d**) A second streaking at 42 °C eliminated plasmids. (**e**) Sanger sequencing was conducted to confirm the *apd* ORF knockout

strains (Fig. 4e). The observations could be attributed to the distinct roles of *nanH* and *apd* in bacterial biological functions, which warranted further investigation. Moreover, variations in the growth curves of the mutants may provide an explanation for why *apd* was knocked out more rapidly and easily than *nanH*.

Plasmid copy number significantly affects the expression of recombination-related proteins

The optimal temperature for *G. parasuis* growth and DNA replication is approximately 37 °C, rather than 30 °C. Therefore, we speculated that 37 °C might be more conducive to homologous DNA recombination. We first evaluated the expression of recombinant genes (*recA*, *recB*, *recC*, *recD*, *and ruvA*) in wild-type CF7066 at 30 °C and 37 °C by RT−qPCR. The results revealed minimal differences in the expression of each gene at

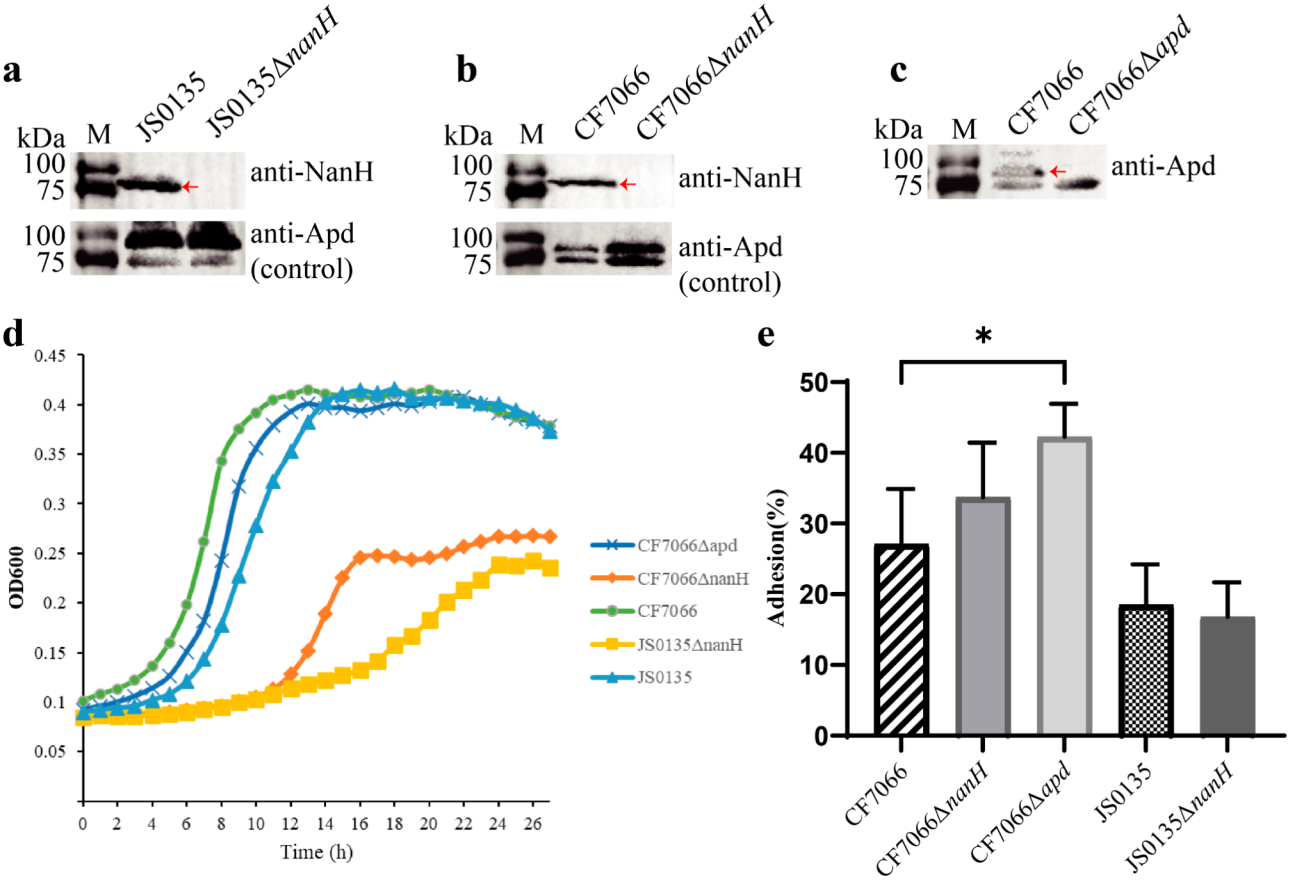

Fig. 4 Characterization of three marker-free knockout mutants. (**a**, **b**) Western blot analysis revealed that NanH was detectable in wild-type JS0135 and CF7066 strains, but not in their respective knockout mutants. (**c**) Similarly, Apd was absent in CF7066Δ*apd*, while it was expressed in wild-type CF7066. Red arrowheads indicate the presence of NanH or Apd in the wild-type strains. (**d**) The bacterial OD_{600} was measured every 30 min to draw the growth curve. Compared to the CF7066 and JS0135 respectively, CF7066Δ*apd* had no effect on growth, but both JS0135Δ*nanH* and CF7066Δ*nanH* exhibited poor growth. (**e**) The adhesion rate of CF7066Δ*apd* increased significantly in contrast to wild-type CF7066, while both CF7066Δ*nanH* and JS0135Δ*nanH* were similar to CF7066 and JS0135 respectively

different temperatures (Fig. 5a). However, in the transformant CF7066 (pSHG5-Δ*apd*), the expression of the recombinant genes was significantly upregulated at 30 °C (Fig. 5b). Specifically, the expression of *recC* was the most obviously upregulated, being approximately 7 times greater than that at 37 °C (Fig. 5b). Moreover, the RT–qPCR results of the bacterial solution indicated that the plasmid copy number at 30 °C was more than twice that at 37 °C (Fig. 5c). This indicated that the plasmid copy number was higher at 30 °C, whiched resulted in greater expression of the recombinant genes. However, the slow growth of colonies at 30 °C was not conducive to recombination, and our previous study had never successfully screened mutants at 30 °C. It can be proposed that within the temperature alternation window, a high plasmid copy number results in the high expression of recombination genes, while bacterial chromosomes maintain efficient replication. Therefore, it can be posited that DNA homologous recombination events are more likely to occur during the temperature alternation window.

Discussion

In previous studies, we attempted to use the method described by Taturn and Briggs [24] to screen for double-crossover strains. In brief, the transformants were first subjected to selection at 42 °C to cure the plasmids, allowing only the single-crossover colonies to grow under selection pressure; then, the single-crossover colonies were propagated on gentamicin-free plates at 30 °C to screen for the knockout strains. However, this method failed in our study because homologous DNA recombination was infrequent during normal cellular metabolism, and target gene knockout conferred a growth disadvantage to the resulting mutants. As a result, the single-crossover strains were more inclined to revert to the wild-type. Moreover, single-crossover strains can only recombine once after the plasmids are cured, which presents a significant challenge in screening procedures.

To address these challenges and increase the likelihood of obtaining double-crossover genotypes, we developed a strategy for culturing transformants alternately at

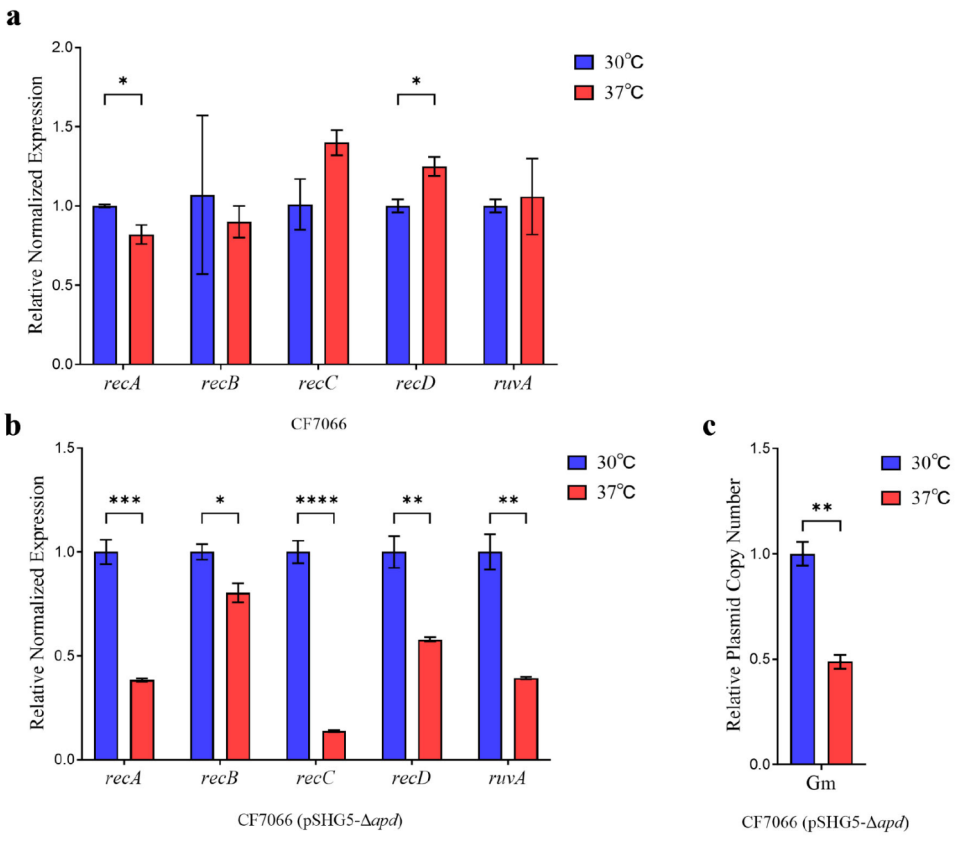

Fig. 5 Transcription levels of DNA recombination-related genes (*recA*, *recB*, *recC*, *recD*, *ruvA*) at different temperatures. (**a**) Transcription levels of various DNA recombination-related genes in the wild-type strain CF7066 at 30℃ and 37℃. (**b**) Transcription levels of various DNA recombination-related genes in the transformant CF7066 (pSHG5-Δ*apd*) at 30℃ and 37℃. (**c**) Plasmid copy numbers of the transformant CF7066 (pSHG5-Δ*apd*) at 30℃ and 37℃

37 °C and 30 °C. Our approach was based on the hypothesis that DNA damage occurs spontaneously during normal cellular metabolism and that double-strand DNA breaks (DSBs) are the most severe type of DNA damage. Homologous recombination is a well-known pathway for repairing DSBs [25, 26] and occurs mainly during DNA replication [27–30]. Therefore, we proposed that a greater copy number of plasmids in cells would lead to more frequent DSBs and consequently activate the repair mechanism more frequently, thus increasing the probability of homologous recombination. This hypothesis was supported by our observations, where the efficiency of gene knockouts improved significantly with the alternating temperature strategy.

Additionally, previous work has shown that recombination is partially dependent on DNA replication [31, 32] and that blocking DNA synthesis by high temperatures reduces the frequency of recombination [32]. We believe that DNA double-strand unwinding before DNA replication provides opportunities for homology searching and DNA strand invasion, which is a key reaction involved in homologous recombination [33]. Which means, in this study, the improvement of the frequency of homologous recombination is dependent upon the efficient replication of both the genome and the temperature-sensitive plasmids. Conversely, *G. parasuis* grew significantly more slowly at 30 °C, demonstrating that DNA synthesis decreases, and the TS plasmid failed to replicate at or above 42 °C in *G. parasuis* [34]. Consequently, culturing transformants alternately at 37 °C and 30 °C could ensure that both the genome and plasmids replicate efficiently, thereby improving the frequency of recombination.

Moreover, the increase in plasmid copy number at the lower temperature of 30 °C likely enhanced the availability of target sequences for homologous recombination. This phenomenon was observed in our study, where the expression of recombinant genes was significantly higher at 30 °C compared to 37 °C, suggesting that the elevated plasmid copy number facilitated higher recombination efficiency. Additionally, the higher plasmid copy number at 30 °C also implies that, at the molecular level, the likelihood of recombination between the homologous arms on the genome and the plasmid increases. This insight provides a deeper understanding of the molecular mechanisms underlying the improved success rate of our optimized knockout system.

Based on these findings, we speculate that the efficiency of homologous recombination in bacteria might

peak during the temperature transition window. Additionally, homologous recombination is one of the adaptive mutation mechanisms that bacteria use to cope with environmental changes [35–38]. Frequent fluctuations in cultivation temperature may potentially stimulate the activation of homologous recombination. We believe that increasing the frequency of temperature transitions might further enhance the recombination efficiency, though this warrants further investigation.

Our findings also highlight the broader implications of this optimized system. By facilitating more efficient gene knockouts, researchers can more rapidly investigate gene function and pathogenic mechanisms in *G. parasuis*. This advancement not only accelerates basic research but also has potential applications in developing targeted treatments and interventions for Glässer's disease. Furthermore, the principles of our approach could be adapted for use in other bacterial species, thereby contributing to the wider field of microbial genetics and pathogenesis research.

Overall, our optimized marker-free knockout system represents a significant advancement in genetic manipulation techniques for *G. parasuis*. By addressing the limitations of previous methods and leveraging the biological principles of homologous recombination, we have developed a more efficient and reliable method for creating gene knockouts. This system paves the way for future studies to explore the complex genetics of *G. parasuis* and develop novel strategies to combat Glässer's disease.

Conclusion

In this study, we successfully established a marker-free knockout system for *G. parasuis* by electrotransforming TS donor plasmids. Our screening process revealed that culturing transformants alternately at 37 °C and 30 °C promoted homologous recombination, making the production and screening of double-crossover mutants more feasible. Our findings also showed that simultaneous single exchange events based on the two different homologous arms of the target gene could occur, resulting in the insertion of two plasmids into the genome. This marker-free knockout system is simple and efficient, requiring no high transformation efficiency, and the plasmid used for transformation is small and requires no additional elements, which is particularly important for *G. parasuis* due to its plentiful and stringent restriction-modification systems. Additionally, the promotion of crossover and recombination observed in the TS mutation system through alternate cultivation at 37 °C and 30 °C may have potential applications in other microorganisms.

Abbreviations

G. parasuis	Glaesserella parasuis
TS	Temperature-sensitive
SG buffer	Sucrose/glycerol buffer
ORF	Open reading frame

Supplementary Information

The online version contains supplementary material available at https://doi.org/10.1186/s12896-024-00887-w.

Supplementary Material 1

Author contributions

Conceived and designed the experiments: J.X. and X.X. Performed the experiments: J.X. and Y.W. Contributed reagents/materials: X.X., D.W., Y.S., X.C., H.C. and H.Z. Wrote the paper: J.X., Y.W., H.Z., and X.X. All authors have reviewed the manuscript.

Funding

This work was funded by the National Key Research and Development Program of China (2022YFD1800902).

Data availability

All data generated or analyzed during this study are included in this published article (and its supplementary information files). All vectors generated in this study can be obtained from the corresponding author upon reasonable request.

Declarations

Ethics approval and consent to participate

This article does not contain any studies with human participants or animals performed by any of the authors.

Consent for publication

Not applicable.

Competing interests

The authors declare no competing interests.

Received: 8 July 2024 / Accepted: 21 August 2024
Published online: 03 September 2024

References

1. Bossé JT, Durham AL, Rycroft AN, Kroll JS, Langford PR. New Plasmid Tools for Genetic Analysis of Actinobacillus pleuropneumoniae and other Pasteurellaceae. Appl Environ Microbiol. 2009;75(19):6124–31. https://doi.org/10.1128/aem.00809-09.
2. Alvarez-Estrada A, Fernando Rodriguez-Ferri E, Martinez-Martinez S, Alvarez B, Fernandez-Caballero T, Dominguez J, Bernardo Gutierrez-Martin C. TLR2, Siglec-3 and CD163 expressions on porcine peripheral blood monocytes are increased during sepsis caused by Haemophilus parasuis. Comp Immunol Microbiol Infect Dis. 2019;64:31–9. https://doi.org/10.1016/j.cimid.2019.02.001.
3. Olvera A, Segales J, Aragon V. Update on the diagnosis of Haemophilus parasuis infection in pigs and novel genotyping methods. Vet J. 2007;174(3):522–9. https://doi.org/10.1016/j.tvjl.2006.10.017.
4. Amano H, Shibata M, Takahashi K, Sasaki Y. Effects on endotoxin pathogenicity in pigs with acute septicemia of Haemophilus parasuis infection. J Vet Med Sci. 1997;59(6):451–5. https://doi.org/10.1292/jvms.59.451.
5. Zhang B, Ku X, Yu X, Sun Q, Wu H, Chen F, Zhang X, Guo L, Tang X, He Q. Prevalence and antimicrobial susceptibilities of bacterial pathogens in Chinese pig farms from 2013 to 2017. Sci Rep. 2019;9. https://doi.org/10.1038/s41598-019-45482-8.
6. Sunaga F, Tsuchiaka S, Kishimoto M, Aoki H, Kakinoki M, Kure K, Okumura H, Okumura M, Okumura A, Nagai M, et al. Development of a one-run real-time PCR detection system for pathogens associated with porcine respiratory diseases. J Veterinary Med Sci. 2019. https://doi.org/10.1292/jvms.19-0063.

7. Macedo N, Rovira A, Torremorell M. Haemophilus parasuis: infection, immunity and enrofloxacin. Vet Res. 2015. https://doi.org/10.1186/s13567-015-0263-3.
8. Zhang P, Hao H, Li J, Ahmad I, Cheng G, Chen D, Tao Y, Huang L, Wang Y, Dai M, et al. The epidemiologic and pharmacodynamic cutoff values of Tilmicosin against Haemophilus parasuis. Front Microbiol. 2016. https://doi.org/10.3389/fmicb.2016.00385.
9. Zhang X, Cai X, Qi Y, Liu Y, Cao Q, Wang X, Chen H, Xu X. Improvement in the efficiency of natural transformation of Haemophilus parasuis by shuttle-plasmid methylation. Plasmid. 2018;98:8–14. https://doi.org/10.1016/j.plasmid.2018.07.001.
10. Chen L, Wu D, Cai X, Guo F, Blackall PJ, Xu X, Chen H. Electrotransformation of Haemophilus parasuis with in vitro modified DNA based on a novel shuttle vector. Vet Microbiol. 2012;155(2–4):310–6. https://doi.org/10.1016/j.vetmic.2011.08.020.
11. Bigas A, Garrido ME, de Rozas AM, Badiola I, Barbe J, Llagostera M. Development of a genetic manipulation system for Haemophilus parasuis. Vet Microbiol. 2005;105(3–4):223–8. https://doi.org/10.1016/j.vetmic.2004.10.015.
12. Zhou Q, Feng S, Zhang J, Jia A, Yang K, Xing K, Liao M, Fan H. Two glycosyltransferase genes of Haemophilus parasuis SC096 implicated in Lipooligosaccharide Biosynthesis, serum resistance, adherence, and Invasion. Front Cell Infect Microbiol. 2016;6:100. https://doi.org/10.3389/fcimb.2016.00100.
13. Eberle KC, Hau SJ, Luan SL, Weinert LA, Stasko JA, Wang J, Peters SE, Langford PR, Rycroft AN, Wren BW, et al. Generation and evaluation of a glaesserella (Haemophilus) parasuis Capsular Mutant. Infect Immun. 2020;88(5). https://doi.org/10.1128/IAI.00879-19.
14. Xiao J, Wang Q, Xiao K, Zhu W, Huang J, Cai X, Chen H, Xu X. Generation of markerless and multiple-gene knockout in Glaesserella parasuis based on natural transformation and flp recombinase. Appl Microbiol Biotechnol. 2022;106(13–16):5167–78. https://doi.org/10.1007/s00253-022-11994-z.
15. Zhang LH, Li Y, Dai K, Wen XT, Wu R, Huang XB, Jin J, Xu K, Yan QG, Huang Y, et al. Establishment of a Successive Markerless Mutation System in Haemophilus parasuis through Natural Transformation. PLoS ONE. 2015;10(5):12. https://doi.org/10.1371/journal.pone.0127393.
16. Fu L, Xie C, Jin Z, Tu Z, Han L, Jin M, Xiang Y, Zhang A. The prokaryotic argonaute proteins enhance homology sequence-directed recombination in bacteria. Nucleic Acids Res. 2019;47(7):3568–79. https://doi.org/10.1093/nar/gkz040.
17. Wang X, Xu X, Wu Y, Li L, Cao R, Cai X, Chen H. Polysaccharide biosynthesis protein CapD is a novel pathogenicity-associated determinant of Haemophilus parasuis involved in serum-resistance ability. Vet Microbiol. 2013;164(1–2):184–9. https://doi.org/10.1016/j.vetmic.2013.01.037.
18. Wang H, Liu L, Cao Q, Mao W, Zhang Y, Qu X, Cai X, Lv Y, Chen H, Xu X, et al. Haemophilus parasuis alpha-2,3-sialyltransferase-mediated lipooligosaccharide sialylation contributes to bacterial pathogenicity. Virulence. 2018;9(1):1247–62. https://doi.org/10.1080/21505594.2018.1502606.
19. Lancashire JF, Terry TD, Blackall PJ, Jennings MP. Plasmid-encoded Tet B tetracycline resistance in Haemophilus parasuis. Antimicrob Agents Chemother. 2005;49(5):1927–31. https://doi.org/10.1128/AAC.49.5.1927-1931.2005.
20. Liu Y, Du Y, Song Y, Tian Y, Qi Y, Zhang Q, He Q, Wang X, Chen H, Cai X, et al. Development and application of an antibody detection ELISA for Haemophilus parasuis based on a monomeric autotransporter passenger domain. Bmc Vet Res. 2019;15(1):436. https://doi.org/10.1186/s12917-019-2128-x.
21. Song Y, Pan Q, Xiao J, Li W, Ma H, Chen H, Cai X, Xu X. Sialidase of Glaesserella Parasuis augments inflammatory response via Desialylation and Abrogation of negative regulation of Siglec-5. Infect Immun. 2021;89(5). https://doi.org/10.1128/IAI.00696-20.
22. Yue M, Yang F, Yang J, Bei W, Cai X, Chen L, Dong J, Zhou R, Jin M, Jin Q et al. Complete genome sequence of Haemophilus parasuis SH0165. J Bacteriol 2009, 191(4):1359–60https://doi.org/10.1128/jb.01682-08
23. Schafer A, Tauch A, Jager W, Kalinowski J, Thierbach G, Puhler A. Small mobilizable multi-purpose cloning vectors derived from the Escherichia coli plasmids pK18 and pK19: selection of defined deletions in the chromosome of Corynebacterium glutamicum. Gene. 1994;145(1):69–73. https://doi.org/10.1016/0378-1119(94)90324-7.
24. Tatum FM, Briggs RE. Construction of in-frame aroA deletion mutants of Mannheimia haemolytica, Pasteurella multocida, and Haemophilus Somnus by using a new temperature-sensitive plasmid. Appl Environ Microbiol. 2005;71(11):7196–202. https://doi.org/10.1128/AEM.71.11.7196-7202.2005.
25. Moynahan ME, Jasin M. Mitotic homologous recombination maintains genomic stability and suppresses tumorigenesis. Nat Rev Mol Cell Biol. 2010;11(3):196–207. https://doi.org/10.1038/nrm2851.
26. Scully R, Panday A, Elango R, Willis NA. DNA double-strand break repair-pathway choice in somatic mammalian cells. Nat Rev Mol Cell Biol. 2019;20(11):698–714. https://doi.org/10.1038/s41580-019-0152-0.
27. Kuzminov A. Single-strand interruptions in replicating chromosomes cause double-strand breaks. Proc Natl Acad Sci U S A. 2001;98(15):8241–6. https://doi.org/10.1073/pnas.131009198.
28. Levy A, Goren MG, Yosef I, Auster O, Manor M, Amitai G, Edgar R, Qimron U, Sorek R. CRISPR adaptation biases explain preference for acquisition of foreign DNA. Nature. 2015;520(7548):505–10. https://doi.org/10.1038/nature14302.
29. Michel B, Flores MJ, Viguera E, Grompone G, Seigneur M, Bidnenko V. Rescue of arrested replication forks by homologous recombination. Proc Natl Acad Sci U S A. 2001;98(15):8181–8. https://doi.org/10.1073/pnas.111008798.
30. Shee C, Cox BD, Gu F, Luengas EM, Joshi MC, Chiu LY, Magnan D, Halliday JA, Frisch RL, Gibson JL, et al. Engineered proteins detect spontaneous DNA breakage in human and bacterial cells. Elife. 2013;2:e01222. https://doi.org/10.7554/eLife.01222.
31. Li X, Heyer WD. Homologous recombination in DNA repair and DNA damage tolerance. Cell Res. 2008;18(1):99–113. https://doi.org/10.1038/cr.2008.1.
32. Stahl FW, McMilin KD, Stahl MM, Nozu Y. An enhancing role for DNA synthesis in formation of bacteriophage lambda recombinants. Proc Natl Acad Sci U S A. 1972;69(12):3598–601. https://doi.org/10.1073/pnas.69.12.3598.
33. Lesterlin C, Ball G, Schermelleh L, Sherratt DJ. RecA bundles mediate homology pairing between distant sisters during DNA break repair. Nature. 2014;506(7487):249–. https://doi.org/10.1038/nature12868.
34. Briggs RE, Tatum FM. Generation and molecular characterization of new temperature-sensitive plasmids intended for genetic engineering of Pasteurellaceae. Appl Environ Microbiol. 2005;71(11):7187–95. https://doi.org/10.1128/AEM.71.11.7187-7195.2005.
35. Torrance EL, Burton C, Diop A, Bobay LM. Evolution of homologous recombination rates across bacteria. Proc Natl Acad Sci U S A. 2024;121(18):e2316302121. https://doi.org/10.1073/pnas.2316302121.
36. Didelot X, Meric G, Falush D, Darling AE. Impact of homologous and non-homologous recombination in the genomic evolution of Escherichia coli. BMC Genomics. 2012;13:256. https://doi.org/10.1186/1471-2164-13-256.
37. Gonzalez-Torres P, Rodriguez-Mateos F, Anton J, Gabaldon T. Impact of homologous recombination on the evolution of Prokaryotic Core genomes. mBio. 2019;10(1). https://doi.org/10.1128/mBio.02494-18.
38. Matic I, Taddei F, Radman M. Survival versus maintenance of genetic stability: a conflict of priorities during stress. Res Microbiol. 2004;155(5):337–41. https://doi.org/10.1016/j.resmic.2004.01.010.

Publisher's note

Springer Nature remains neutral with regard to jurisdictional claims in published maps and institutional affiliations.